SCIENTIFIC REP😊RTS

OPEN

Large enhancement of superconducting transition temperature in single-element superconducting rhenium by shear strain

Masaki Mito[1], Hideaki Matsui[1], Kazuki Tsuruta[1], Tomiko Yamaguchi[1], Kazuma Nakamura[1], Hiroyuki Deguchi[1], Naoki Shirakawa[2], Hiroki Adachi[3], Tohru Yamasaki[3], Hideaki Iwaoka[4], Yoshifumi Ikoma[4] & Zenji Horita[4,5]

Finding a physical approach for increasing the superconducting transition temperature (T_c) is a challenge in the field of material science. Shear strain effects on the superconductivity of rhenium were investigated using magnetic measurements, X-ray diffraction, transmission electron microscopy, and first-principles calculations. A large shear strain reduces the grain size and simultaneously expands the unit cells, resulting in an increase in T_c. Here we show that this shear strain approach is a new method for enhancing T_c and differs from that using hydrostatic strain. The enhancement of T_c is explained by an increase in net electron–electron coupling rather than a change in the density of states near the Fermi level. The shear strain effect in rhenium could be a successful example of manipulating Bardeen–Cooper–Schrieffer-type Cooper pairing, in which the unit cell volumes are indeed a key parameter.

Single-element superconductors are Bardeen–Cooper–Schrieffer (BCS)-type superconductors, and volume shrinkage under applied pressure (P) is known to be an effective approach to manipulating the superconducting transition temperature (T_c)[1]. When the superconductors are subjected to high pressure, important changes occur in both the conduction electron state and lattice vibration. The change in T_c under hydrostatic contraction, in which the strain tensor has only diagonal components, is not uniform; in simple metals such as Al, Zn, Ga, Cd, In, Sn, Hg, and Pb, T_c decreases under pressure, whereas in those such as V, Zr, and Tl, T_c increases under pressure[1,2]. According to the McMillan–Allen–Dynes formula, T_c can be expressed on a quantitative basis as

$$T_c = \frac{\omega_{\ln}}{1.2} \exp\left[-\frac{1.04(1 + \lambda)}{\lambda - \mu^*(1 + 0.62\lambda)}\right]$$

(1)

where $\omega_{\ln}$ is the phonon frequency, λ is the electron lattice coupling, and μ^* is the effective Coulomb potential[3,4]. However, the change in T_c under pressure in simple metals can be understood more concretely using the following formula,

$$T_c \approx \sqrt{\frac{k}{M}} \exp\left[-\frac{k}{N(E_F) <I^2>}\right]$$

(2)

[1]Faculty of Engineering, Kyushu Institute of Technology, Kitakyushu 804-8550, Japan. [2]Flexible Electronics Research Center (FLEC), National Institute of Advanced Industrial Science and Technology (AIST), Tsukuba 305-8565, Japan. [3]Graduate School of Engineering, University of Hyogo, Himeji 671-2280, Japan. [4]Department of Materials Science and Engineering, Faculty of Engineering, Kyushu University, Fukuoka, 819-0395 Japan. [5]International Institute for Carbon-Neutral Energy Research (WPI-I2CNER), Kyushu University, Fukuoka, 819-0395 Japan. Correspondence and requests for materials should be addressed to M.M. (email: mitoh@mns.kyutech.ac.jp)

where M is the mass of the ions, k is the spring constant, $N(E_F)$ is the electronic-density of states at the Fermi level E_F, and $<I^2>$ is the average square electronic matrix element[1,2]. The product of $N(E_F)$ and $<I^2>$ is an electronic term called as the Hopfield parameter η[5]. In equation (2), any change in the pre-factor is negligible compared to the terms in the exponent. The relative magnitudes of the increases in k and η determine whether T_c will increase or decrease under pressure. Thus, the decrease in T_c with pressure in simple metals originates mainly from the increase in k, *i.e.*, lattice stiffening. Thus, in simple metals with d $T_c/dP < 0$, the hydrostatic strain effects are understood to be governed by stiffening in the lattice vibration spectrum rather than the changes in the electronic properties such as broadening of the density of states near the Fermi level[1,2]. Here, the electron-lattice coupling parameter λ in equation (1) is expressed as $\lambda = N(E_F)<I^2>/M<\omega^2>$, where $<\omega^2>$ is the average square phonon frequency. Further, it is also thought that the decrease in T_c with pressure in simple metals results from a weakening of λ due to the shift of the phonon spectrum to higher frequencies[1]. Interestingly, the hydrostatic pressure effect in rhenium (Re) is unique in that the T_c exhibits a decrease followed by an increase with a minimum at approximately 0.6 GPa[6,7].

In high-pressure studies, the exploitation of the isotropic features of stress, i.e., hydrostatic pressure, has been viewed as an ideal structural manipulation; the intrinsic response to stress has been studied, and first-principles calculations have been performed. As mentioned above, under hydrostatic pressure conditions, only diagonal components exist in the strain tensor. Indeed, hydrostatic pressure is especially important in the development of organic superconductors, in which nondiagonal components are detrimental to the strain-induced superconductivity[8]. However, in this study of Re, we present a new approach for greatly increasing T_c, in which shear stress instead of hydrostatic pressure is a key parameter affecting the T_c value of superconductors.

Previous studies of the strain effects in Re are briefly reviewed here. According to an earlier study of Re by Hulm and Goodman in 1957, an arc-melted powder without strain has a sharp superconducting transition at $T_c = 1.70$ K[9]. The Meissner effect reveals the magnetic-field-dependent characteristics of typical type-I superconductors. They also reported that Re ground to a cylinder has a T_c value of 2.7 K, suggesting that some shear strain effect could work positively to increase T_c. However, when pure Re crystals with T_c of 1.69–1.70 K are placed under hydrostatic pressure, T_c decreases with a slope of $dT_c/dP \sim -2 \times 10^{-2}$ K/GPa for $P < 0.4$ GPa, and the initial slope corresponds to approximately -1×10^{-2} K at a volume shrinkage of 0.1%[6,7]. The change in T_c is found to increase at around 0.6 GPa, where T_c has the decrease of approximately 0.01 K. For $P > 1.6$ GPa, the increase in T_c tends to saturate at $T_c \sim 1.69$ K. Thus, the effect of shear strain in Re is completely different from the hydrostatic pressure effects described above, but is instead qualitatively consistent with the effects of doping with Os or W[10]. Generally, the shear strain reduces the domain size; hence it is not considered a promising factor for physical manipulation. Here, we consider the shear strain effect in Re using the proposed new approach.

The experimental apparatus for our high-pressure experiments was a diamond anvil cell[11]. A gasket was clamped between two diamond anvils. The gasket material must be hard and resistant to any stress. In fact, Re is often used as a gasket material. From our experience, we have found that a Re gasket often has a T_c above 2.0 K, and T_c depends on the degree of prior treatment (that is, it is related to the magnitude of internal strain in the gasket). Indeed, this phenomenon is the same as the strain effect reported by Hulm and Goodman[9]. Given the above background, we systematically study the effect of shear strain on the superconductivity of Re over a wide strain range.
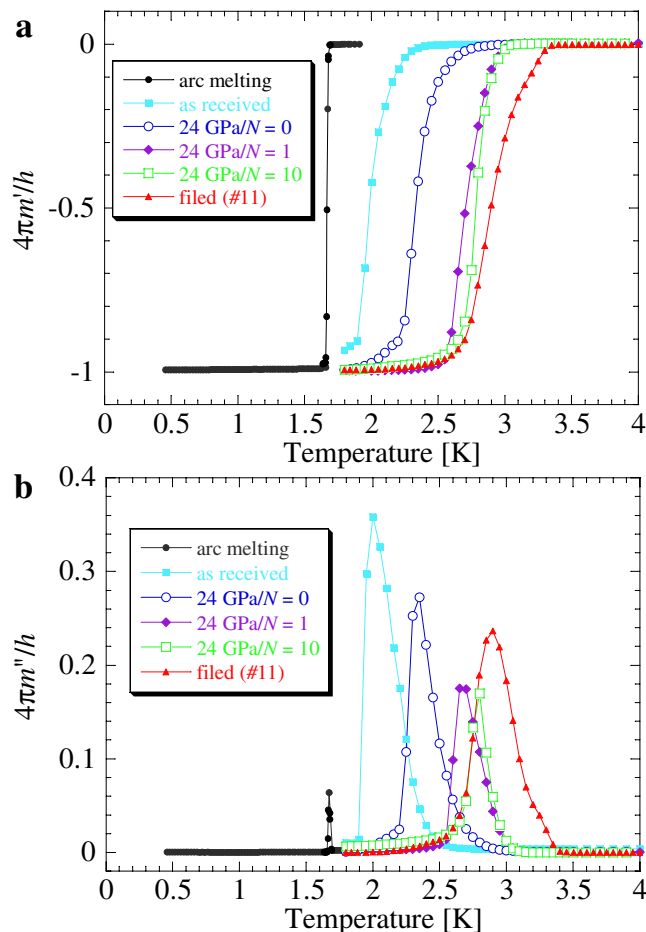
Severe plastic deformation can be used to apply a large strain to materials, resulting in bulk nanostructured materials with ultrafine-grained structures[12]. Examples of such deformation include equal-channel angular pressing[13], accumulative roll-bonding[14], and high-pressure torsion (HPT)[15]. In 1935, Bridgman introduced the HPT method combined with hydrostatic pressure as a method for obtaining high shearing stress[16]. In particular, this HPT method can introduce intense shear strain so that the materials have ultrafine grains on the submicrometer or nanometer scale[15,17–19]. In the present study, the HPT method is adopted to apply intense shear strain to Re. The shear strain effects are physically elucidated using structural analysis and first-principles calculations.

Results

Magnetic measurements.
The in-phase and out-of-phase ac magnetic susceptibility (denoted by $4\pi m'/h$ and $4\pi m''/h$, respectively) as a function of temperature (T) for the arc-melted sample are shown in Fig. 1(a,b), respectively, and Fig. 2(a) shows the magnetization (M) as a function of the dc magnetic field (H). At around 1.7 K, a sharp Meissner signal appeared within a temperature width of 20 mK, and T_c was estimated to be 1.7 K. We confirmed that in a spherical sample of arc-melted material, an almost perfect Meissner signal appeared. In the disk samples, a Meissner signal with a similar magnitude was observed. The magnetization $M(H)$ exhibited a sharp jump at around $H = 170 \pm 30$ Oe, indicating that the unstrained sample was a type-I superconductor. The results are consistent with those reported by Hulm and Goodman[9].

Figure 1 also shows the temperature dependence of the in-phase and the out-of-phase ac susceptibility for HPT-processed Re. In the $4\pi m'/h$ data, the Meissner signal shifted toward the high-temperature side with increasing strain. When we evaluated T_c according to the onset of $4\pi m'/h$, T_c was estimated to be 2.5, 2.9, and 3.0 K for $N = 0$, 1, and 10, respectively, where N is the number of revolutions in the HPT process. For reference, the T_c value of the as-received sample was 2.2 K. We recognize a large enhancement of T_c caused by torsion. The susceptibility $4\pi m''/h$ reveals the energy loss against the ac magnetic field and the distribution of T_c. The peak of $4\pi m''/h$ corresponds to the midpoint of a large decrease in $4\pi m'/h$. The upper limit of a finite m'' corresponds to a possible optimal T_c. Even at $N = 0$, the optimal T_c of about 2.8 K implies the possibility of increasing T_c. The possible T_c for $N = 10$ is 3.2 K. We confirmed that the possible T_c of Re was enhanced to 3.4 K when the sample was filed using sandpapers as shown in Fig. S4, suggesting the importance of using shear strain instead of hydrostatic compression.

Figure 2(b–d) shows $M(H)$ for the HPT-processed Re at $T < T_c$. The field region of the Meissner signal was greatly enhanced with increasing N, and the type of superconductivity, determined by extracting the magnetic
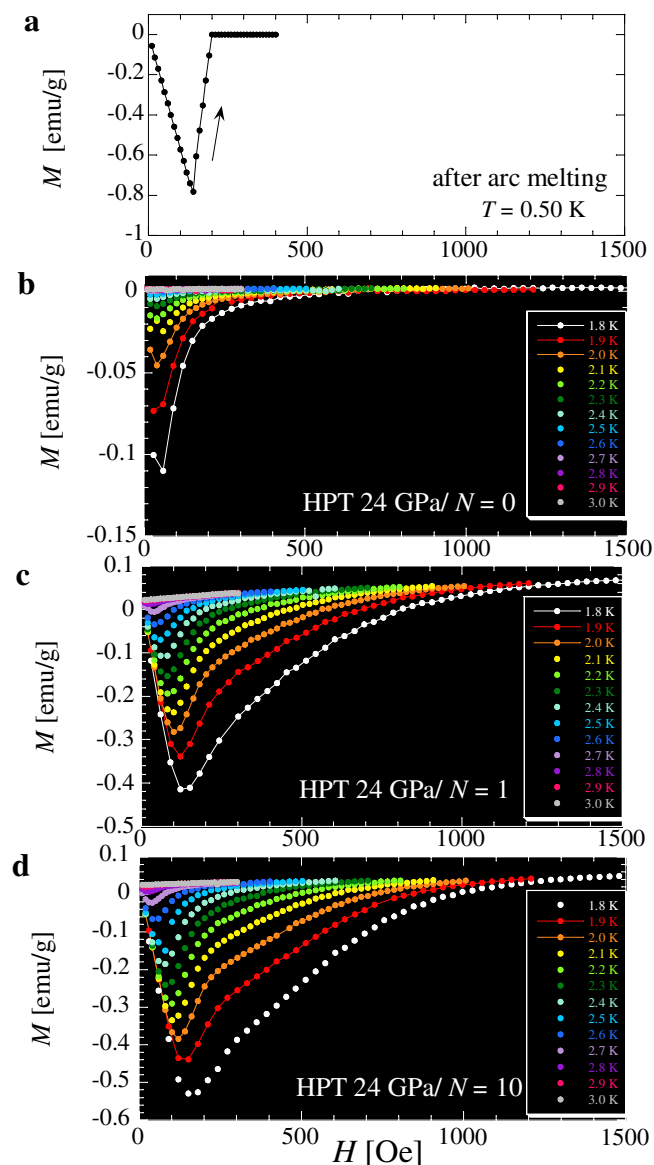
Figure 1. Temperature dependence of the (**a**) in-phase ac susceptibility $4\pi m'/h$ and (**b**) out-of-phase one $4\pi m''/h$ for Re processed by HPT at 24 GPa with $N = 0$, 1, and 10. The in-phase susceptibility is shown in SI units in order to evaluate the volume fraction. Data for the arc-melted and as-received samples are also shown for reference.

flux, changed from type-I to type-II. At $T = 1.8$ K, the lower critical field H_{c1} is less than 30, 90, and 130 Oe for $N = 0$, 1, and 10, respectively. Furthermore, the upper critical field H_{c2} at $T = 1.8$ K is 0.7, 1.3, and >1.5 kOe for $N = 0$, 1, and 10, respectively. Thus, a reduction in the coherence length ξ was experimentally suggested by the change in the magnetic field dependence of the Meissner signal as well as the change in T_c ($\propto \xi^{-1}$). The positive effect of the shear strain appears in the increases in H_{c1} and H_{c2} as well as T_c.
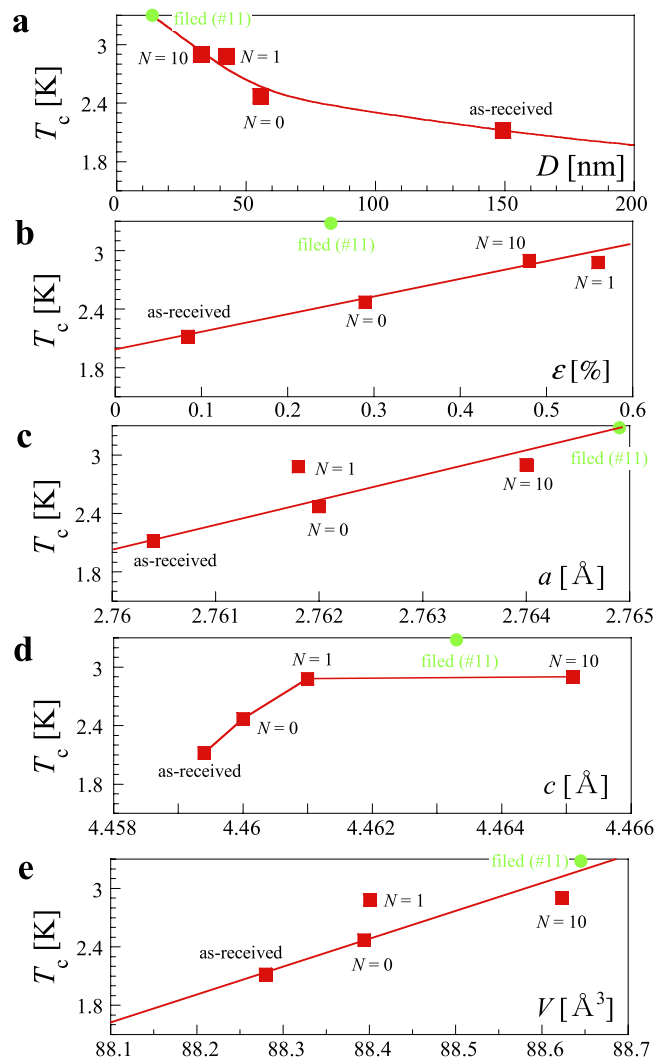
Structural characterization. Figure S2 shows the X-ray diffraction profiles of the as-received and HPT-processed samples. The shift in a series of diffraction peaks yields information about the lattice parameters. The half-width of the diffraction peaks indicates the average grain size and internal strain. Figure 3 shows the relation between T_c and several structural parameters; the crystalline size D (a), crystalline strain ε (b), lattice parameters a (c) and c (d), and unit cell volume V (e). These figures include data for the as-received specimen, the HPT-processed ones ($N = 0$, 1, and 10 at $P = 24$ GPa), and a filed specimen (#11 in Table S1). The filing was performed under a slight stress along the direction perpendicular to the disk, and the sample was subjected to strong strain caused by rotation. The shear strain accompanying rotation on the c-plane was thought to expand the size of the c-plane and decrease the crystalline size. As the shear strain increased, expansion along the a-axis also occurred, resulting in an increase in the unit cell volume. Indeed, the largest expansion along the a-axis was observed in the filed Re rather than the HPT-processed Re with $N = 10$. According to the results for the as-received, HPT-processed, and filed specimens, D, a, and V are promising parameters for scaling T_c. Figure S3 shows a transmission electron microscopy micrograph of the sample processed by HPT at $P = 24$ GPa and $N = 10$. The grain size was reduced to the order of ~100 nm, suggesting a reduction in the coherence length. As shown in Fig. 1, a prominent Meissner signal was observed, and the present materials were considered to be strongly coupled superconducting-grain systems.

Band structure calculations. To see the effect of changes in the electronic structures, we performed band structure calculations for Re with different configurations. Figure 4(a) shows the calculated ab-initio band structure for an experimental structure with $a = 2.758$ Å and $c = 4.447$ Å, and Fig. 4(b) compares the densities of states for different lattice parameters. A slight lattice expansion (around 1%) gave rise to appreciable overall shrinkage

Figure 2. (**a**) Magnetization M as a function of dc magnetic field (H) for the arc-melted sample. (**b**–**d**) Temperature dependence of M for HPT-treated Re for (**b**) $N = 0$, (**c**) $N = 1$, and (**d**) $N = 10$. M is evaluated using CGS units in order to extract the shift of the Meissner signal.

of the density of states toward to the Fermi level ($E = 0$) (thin red to thick blue curves). In particular, a shift of the peak around 5 eV was noticeable. These observations indicate a lowering of the excitation energy caused by volume expansion. In many-body perturbation theory[20–22], the lowering of the excitation energy is generally associated with enhancement of the polarization function. This polarization enhancement, i.e., the large dielectric screening, can weaken the effective repulsion between electrons. We thus expect the electronic pseudopotential μ and also μ^* to reduce with volume expansion. In addition, we see in the inset in panel (b) that the density of states at the Fermi level increases with volume expansion. In 5d metals, the increase in the density of states at the Fermi level can generally lead to enhancement of the electron-phonon coupling λ[3]. The change in these parameters supports reasonably well the presented experimental observation that volume expansion (i.e., the shear strain) leads to an enhancement of T_c. We note that the same tendency was observed in alkali-doped C_{60} systems[23]. Moreover, it is known that Re uniquely exhibits an increase in T_c (at maximum, 2.2 K) when some Re is replaced with Os or W, in which the electronic density of states increases just below the Fermi level[10]. According to Chu *et al.*, the change in the T_c value of Re with alloying can be understood in terms of a change in λ[10]. The present results are reasonably consistent with the effect of replacing some Re with Os or W, where the former exhibits a more drastic increase in T_c.
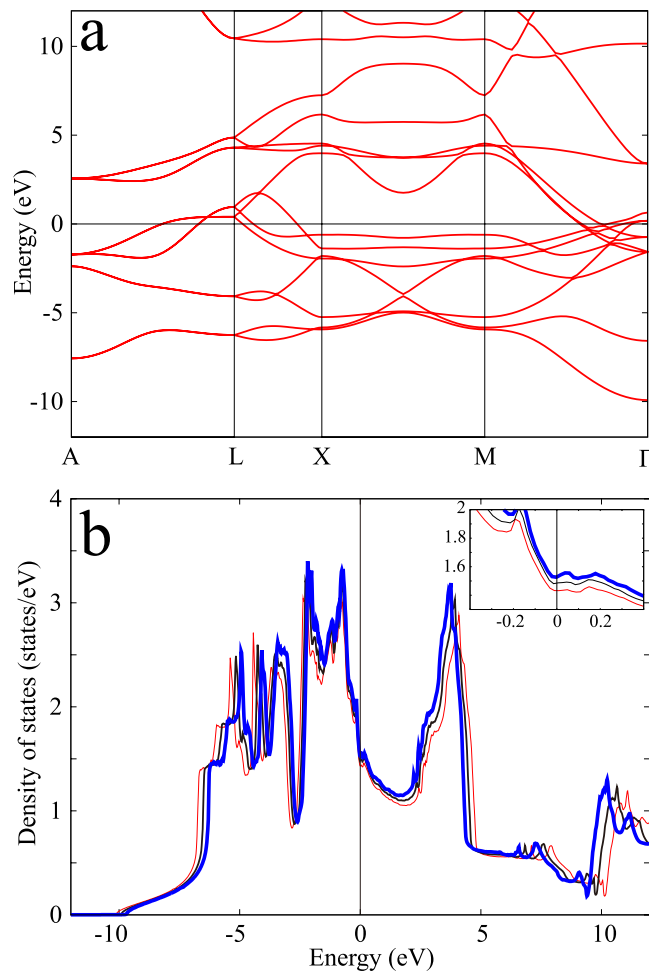
Figure 3. Relation between T_c and the following structural parameters; (**a**) crystalline size D, (**b**) crystalline strain ε, the lattice parameters (**c**) a, (**d**) c, and (**e**) unit cell volume V. A series of experimental data was obtained for the as-received, HPT-treated, and filed specimens.

Discussion

Here we discuss some factors that could be promising for increasing T_c. According to the BCS theory, T_c increases as the density of states at the Fermi level increases, because the number of electron pairs contributing to the super-conductivity increases there. Furthermore, according to the MAD formula in equation (1), T_c increases as the pho-non frequency becomes higher and the electron-phonon interaction becomes larger. In previous high-pressure experiments on single-element superconductor**s**, much attention was given to changes in the phonon stiffening as well as the density of states. In the present work, the most important factor is the electron-phonon interaction. This tendency is unique in a series of high-strain experiments on single-element superconductor**s**, suggesting a new approach to modifying T_c. Under hydrostatic pressure, T_c decreases with a slope of approximately -1×10^{-2} K for a volume shrinkage of 0.1%[6,7]. However, in the HPT process including shear strain, T_c increases with a slope of 1.5 K for a volume expansion of 0.7%, which is more than 20 times the change rate under hydrostatic pressure[6,7]. Thus, the effect of shear strain is expected to be a promising factor in enhancing T_c.

In conclusion, Re subjected to HPT has an ultrafine structure in which the grain size decreases to below the submicrometer level and the lattice expands. The superconducting transition temperature T_c increases with increasing strain, and an important strain component here is shear instead of hydrostatic compression. According to first-principles calculations, the density of states at the Fermi energy increases only slightly, but the van-Hove-singularity shifts toward the low-energy side, suggesting enhanced screening. This means that elec-trons are affected by fluctuation of the lattice, resulting in an increase in the electron-phonon coupling. Thus, a change in the electron-phonon coupling instead of the density of states at the Fermi level gives rise to an increase in T_c.

Figure 4. (**a**) Density-functional band structure calculated for an experimental Re structure with $a = 2.758\,\text{Å}$ and $c = 4.447\,\text{Å}$. (**b**) Effect of the lattice change on the density of states, where we scale the lattice parameters by the factor α. Thin-red, black, and thick-blue curves indicate the results for $\alpha = 0.99$, 1, and 1.01, respectively. The results near the Fermi level ($E = 0$) are enlarged in the inset. An overall shrinkage of the density of states toward the Fermi level ($E = 0$) was observed because of a lattice expansion of 1%. The Fermi surfaces for $\alpha = 0.99$, 1.00, and 1.01 are shown in Fig. S5.

Methods

Materials. High-purity Re disks (99.97%, Johnson Mathey) with 4 mm in diameter and 0.25 mm in thickness were subjected to HPT processing under a pressure of $P = 24\,\text{GPa}$ for the revolution number of HPT process $N = 0$, 1, and 10 turns, as shown in Fig. S1. Tool steel was used for the anvils for $N = 0$ and 1, and tungsten carbide was used for $N = 10$. The pressure of 24 GPa is the value given by the applied load, 50 tons, divided by the total area of the central shallow hole made on the anvils, $(2.5\,\text{mm})^2\pi$. This pressure may be slightly overestimated if a burr is formed during the processing. When we used tungsten carbide anvils, processing was feasible without breaking them. Note that not only the strength of the anvils but also the geometry is important for maintaining feasible processing. The strain imposed on the sample was estimated by $\varepsilon = 2\pi\, r\, N / \sqrt{3}\ t$ (where r is the radius and t is the thickness) as the equivalent strain[24,25]. The shear strain generated by HPT processing typically decreases the grain size and thus increases the grain boundary area. As a reference sample, a ball-like sample, whose residual strain was removed, was prepared by sufficient arc melting. Furthermore, for another reference, a Re plate was filed by sandpapers to introduce random shear strain under a small stress perpendicular to the disk. The number of times the plate was filed is denoted by n (the detailed experimental data are shown in the supplemental material). Indeed, the HPT effect has already been studied for other single-element superconductors; a type-II superconductor, niobium (Nb), with $dT_c/dP = -16$ to $-25\,\text{mK/GPa}$ at low pressures, has a maximum T_c of approximately 10 K at around 10 GPa[26]. However, Nb prepared by HPT (6 GPa) exhibits an increase in T_c of only ~0.10 K at maximum[27]. On the other hand, a thin film with a 100 nm thickness under hydrostatic pressure exhibits an increase in T_c with $dT_c/dP = 73\,\text{mK/GPa}$ even at a low pressure[28]. The HPT effect in Nb is qualitatively consistent with the hydrostatic pressure effect in a Nb film. Given the above background, the HPT effect in Re with $T_c > 1.5\,\text{K}$ reported herein is relatively large; hence, we need to understand the effects of the nondiagonal as well as diagonal components of the strain tensor.

Magnetic measurements.   The superconducting transition was investigated by observing the Meissner signal in the ac magnetic susceptibility using a superconducting quantum interference device magnetometer (Quantum Design Inc.) equipped with an ac measurement option and a ^{3}He refrigerator option (IQUANTUM)[29]. The frequency and amplitude (h) of the ac magnetic field were 10 Hz and 4 Oe, respectively. In the ac magnetic susceptibility measurements, the data for the magnetization M were gathered as a function of time t. Fourier analysis of the $M(t)$ data yields the amplitudes of both the in-phase component (m') and that of the out-of-component (m''). Both m' and m'' are divided by the amplitude of the ac field (h) to obtain the ac magnetic susceptibility. For the spherical sample of arc-melted material, the demagnetization field effect was calibrated using a demagnetization coefficient of 1/3, and we obtained a value of 99.4% as the volume fraction of the superconductor. To reduce the diamagnetic effect, the disks of the HPT-treated and filed specimens were placed so that the normal vectors of their round surfaces were perpendicular to the dc magnetic field. The stability of superconductivity in a magnetic field was investigated using the dc magnetic measurement.

X-ray diffraction (XRD).   The grain size, strain, and unit cell parameters were investigated in XRD experiments using an X-ray diffractometer (Rigaku, SmartLab) with Cu-Kα radiation at 45 kV and 200 mA. The grain size and strain were calculated from the integrated intensities of the diffracted peaks using Williamson-Hall analysis[30].

Transmission electron microscopy (TEM).   Microstructural observation was performed using TEM, and the grain size was measured using dark-field images. The grain size estimated by XRD is generally smaller than that measured by TEM.

Band calculation.   Density-functional band structure calculations were performed for several lattice configurations of Re to study the structural change effect on the low-energy electronic structures. Then, first-principles calculations were performed using the Tokyo Ab-initio Program Package[31] with plane-wave basis sets, where norm-conserving pseudopotentials[32,33] and the generalized gradient approximation of the exchange-correlation potential[34] with partial core correction were employed. The cutoff energies for the wave function and charge densities are 49 and 196 Ry, respectively, and $41 \times 41 \times 41$ k-point sampling was employed. The integral over the Brillouin zone was evaluated by the tetrahedron method with a broadening of 0.01 eV. The density of states for Re at the Fermi energy ($E = 0$) is estimated to be 1.486/eV, which is equivalent to 0.372 (eV·spin·atom)$^{-1}$. This value is consistent with the value of 0.33 (eV·spin·atom)$^{-1}$ in McMillan's study[3]. We also calculated the Fermi surface[35] to see the volume change effect on the electronic structure.

References

1. Schilling, J. S. *High-Pressure Effects in Handbook of* High-Temperature *Superconductivity* edited by J. R. Schrieffer (Springer, New York, 2007).
2. Hamlin, J. J. Superconductivity in the metallic elements at high pressures. *Physica* C **514,** 59–76 (2015).
3. McMillan, W. L. Transition temperature of strong-coupled superconductors. *Phys. Rev.* **167,** 331–344 (1968).
4. Allen, P. B. & Dynes, R. C. Transition temperature of strong-coupled superconductors reanalyzed. *Phys. Rev.* **B12,** 905–922 (1975).
5. Hopfield, J. J. On the systematics of high T_c in transition metal materials. *Physica* **55,** 41–49 (1971).
6. Chu, C. W., Smith, T. F. & Gardner, W. E. Superconductivity of rhenium and some rhenium-osmium alloy s at high pressure. *Phys. Rev. Lett.* **20,** 198–201 (1968).
7. Chu, C. W., Smith, T. F. & Gardner, W. E. Study of Fermi-surface topology changes in rhenium and dilute Re solid solutions from T_c measurements at high pressure. *Phys. Rev.* **B1,** 214–221 (1970).
8. Campos, C. E. *et al.* Uniaxial-stress-induced superconductivity in organic conductors. *Phys. Rev.* **B52,** R7014–R7017 (1995).
9. Hulm, J. K. & Goodman, B. B. Superconducting Properties of Rhenium, Ruthenium, and Osmium. *Phys. Rev.* **106,** 659–671 (1957).
10. Chu, C. W., McMillan, W. L. & Luo, H. L. Superconductivity of Re-Os, Re-Ru, Ru-Os, and Re-W hcp alloy systems and slightly doped Re. *Phys. Rev.* **B3,** 3757–3762 (1971).
11. Eremets, M. *High Pressure Experimental Methods* (Oxford University Press, New York, 1996).
12. Valiev, R. Z. *et al.* Producing Bulk Ultrafine-Grained Materials by Severe Plastic Deformation. *JOM* **58,** 33–39 (2006).
13. Segal, V. M., Drobyshevskii, V. I. A. E. & Kopylov, V. I. Plastic working of metals by simple shear. *Russian Metal* **1,** 99–105 (1981).
14. Saito, Y., Utsunomiya, H., Tsuji, N. & Sakai, T. Novel ultra-high straining process for bulk materials-development of the accumulative roll-bonding (ARB) process. *Acta Mater.* **47,** 579–583 (1999).
15. Smirnova, N. A. *et al.* Evolution of the structure of f.c.c.single crystal subjected to strong plastic deformation. *Fiz. Metal. Metalloved.* **61,** 1170–1177 (1986).
16. Bridgman, P. W. Effects of High Shearing Stress Combined with High Hydrostatic Pressure. *Phys. Rev.* **48,** 825–847 (1935).
17. Harai, Y., Ito, Y. & Horita, Z. High-pressure torsion using ring specimens. *Scripta Mater.* **58,** 469–472 (2008).
18. Edalati, K. & Horita, Z. High-pressure torsion of pure metals: Influence of atomic bond parameters and stacking fault energy on grain size and correlation with hardness. *Acta Mater.* **59,** 6831–6836 (2011).
19. Edalati, K. & Horita, Z. Correlations between hardness and atomic bond parameters of pure metals and semi-metals after processing by high-pressure torsion. *Scripta Mater.* **64,** 161–164 (2011).
20. Nakamura, K., Arita, R. & Imada, M. Ab initio Derivation of Low-Energy Model for Iron-Based Superconductors LaFeAsO and LaFePO. *J. Phys. Soc. Jpn.* **77,** 093771 (2008).
21. Nakamura, K., Nohara, Y., Yoshimoto, Y. & Nomura, Y. Ab initio GW plus cumulant calculation for isolated band system: Application to organic conductor (TMTSF)$_2$PF$_6$ and transition-metal oxide SrVO$_3$. *Phys. Rev.* B **93,** 085124 (2016).
22. Akashi, R., Nakamura, K., Arita, R. & Imada, M. High-temperature superconductivity in layered nitrides β-LixM NCl ($M =$ Ti, Zr, Hf): Insights from density functional theory for superconductors. *Phys. Rev.* B **86,** 054513 (2012).
23. Ganin, A. Y. *et al.* Bulk superconductivity at 38K in a molecular system. *Nature Materials* **7,** 367–371 (2008).
24. Wetscher, F., Vorhauer, A., Stock, R. & Pippan, R. Structural refinement of low alloyed steels during severe plastic deformation. *Mater. Sci. Eng.* **A387–389,** 809–816 (2004).
25. Hebesberger, T., Stüwe, H. P., Vorhauer, A., Wetcher, F. & Pippan, R. Structure of Cu deformed by high pressure torsion. *Acta Mater.* **53,** 393–402 (2005).
26. Smith, T. F. Pressure dependence of the superconducting transition for niobium. *Phys. Lett.* A **33,** 465–466 (1970).
27. Nishizaki, T., Lee, S., Horita, Z., Sasaki, T. & Kobayashi, N. Superconducting properties in bulk nanostructured niobium prepared by high-pressure torsion. *Physica* C **493,** 132–135 (2013).

28. Pristáš, G. *et al.* Influence of hydrostatic pressure on superconducting properties of niobium thin film. *Thin Solid Films* **556,** 470–474 (2014).
29. Shirakawa, N. & Tamura, M. Low temperature static magnetization of an organic ferromagnet, β-p-NPNN. *Polyhedron* **24,** 2405–2408 (2005).
30. Williamson, G. K. & Smallman, R. E. Dislocation densities in some annealed and cold-worked metals from measurements on the X-ray debye-scherrer spectrum. *Philos. Mag.* **1,** 34–46 (1956).
31. Yamauchi, J., Tsukada, M., Watanabe, S. & Sugino, O. First-principles study on energetics of *c*-BN(001) reconstructed surfaces. *Surface Science* **341,** L1037–L1041 (1995).
32. Troullier, N. & Martins, J. L. Efficient pseudopotentials for plane-wave calculations. *Phys. Rev.* B **43,** 1993–2006 (1991).
33. Kleinman, L. & Bylander, D. M. Efficacious Form for Model Pseudopotentials. *Phys. Rev. Lett.* **48,** 1425–1428 (1982).
34. Perdew, J. P., Burke, K. & Ernzerhof, M. Generalized Gradient Approximation Made Simple. *Phys. Rev. Lett.* **77,** 3865–3868 (1996).
35. Kawamura, M., Gohda, Y. & Tsuneyuki, S. Improved tetrahedron method for the Brillouin-zone integration applicable to response functions. *Phys. Rev.* B **89,** 094515 (2014).

Acknowledgements

Author Contributions

M.M., H.M., K.T. and H.D. carried out the magnetic measurements above 1.8 K, and prepared the filed specimens. H.I., Y.I. and Z.H. prepared HPT specimens and performed the transmission electron microscopy measurements. N.S. performed the magnetic measurements below 1.8 K. H.A. and T. Yamasaki carried out the structural determination. T. Yamaguchi conducted the arc melting of the filed specimens. K.N. performed the first-principles calculations. M.M. prepared the manuscript with editing by K.N., H.A., H.D. and Z.H. All the authors discussed the results and commented on the manuscript. M.M. and Z.H. supervised all of the work.

Additional Information

Supplementary information accompanies this paper at http://www.nature.com/srep

Competing financial interests: The authors declare no competing financial interests.

How to cite this article: Mito, M. *et al.* Large enhancement of superconducting transition temperature in single-element superconducting rhenium by shear strain. *Sci. Rep.* **6**, 36337; doi: 10.1038/srep36337 (2016).

Publisher's note: Springer Nature remains neutral with regard to jurisdictional claims in published maps and institutional affiliations.